Grazing collisions of gravitational shock waves and entropy production in heavy ion collisions

Shu Lin* and Edward Shuryak†

Department of Physics and Astronomy, SUNY, Stony Brook, New York 11794, USA

(Received 23 February 2009; published 11 June 2009)

AdS/CFT correspondence is now widely used for the study of strongly coupled plasmas, such as those produced in ultrarelativistic heavy ion collisions at the Relativistic Heavy Ion Collider. While properties of equilibrated plasma and small deviations from equilibrium are by now reasonably well understood, the plasma's initial formation and thermal equilibration is a much more challenging issue which remains to be studied. In the dual gravity language, these problems are related to the formation of bulk black holes, and studying trapped surfaces, as we do in this work, is a way to estimate the properties (temperature and entropy) of such black holes. Extending the work by Gubser *et al.* for central collisions, we find numerically trapped surfaces for *noncentral* collisions of ultrarelativistic black holes (gravitational shock waves) with different energies. We observe that beyond a certain critical impact parameter, the trapped surface does not exist, and we argue that there are some experimental indications for a similar jump in entropy production as a function of the impact parameter in real heavy ion collisions. We also present a simple solvable example of the so-called wall-on-wall collision, for colliding objects that depend on the holographic coordinate only. Finally, we critically discuss the applicability of the AdS/CFT approach to real-world heavy ion collisions.

DOI: 10.1103/PhysRevD.79.124015 PACS numbers: 04.70.Bw

I. INTRODUCTION

The quark gluon plasma (QGP) produced in the Relativistic Heavy Ion Collider (RHIC) at Brookhaven National Laboratory is believed to be strongly coupled [1], as evidenced by its rapid equilibration, strong collective flows well reproduced by hydrodynamics, and strong jet quenching. Applications of AdS/CFT correspondence [2,3] to strongly coupled QGP have generated many fundamental results [4–7]; for some further results see [8] for a recent review. However, the progress so far has been mostly related either to equilibrium properties of the plasma, or to kinetics/hydrodynamics close to equilibrium.

The challenging issues related to the violent initial stage of the collisions, in which the QGP is formed and equilibrated, producing most of the entropy, are not yet understood. One issue worth mentioning is the strikingly different views on equilibration held in statistical mechanics on one hand, and in AdS/CFT-based dual gravity on the other. Statistical/kinetic approaches treat equilibration and entropy production as a gradual deformation of particle distributions, from some initial nonthermal state toward the final equilibrated one. In the dual gravity setting the sources of temperature and entropy are both attributed to the gravitational horizons. They may or may not be produced in a collision: For example, by decreasing the collision energy or increasing the impact parameter, one may reach a point at which no horizons are formed. This implies certain singularities, or a view that a switching in equilibration is similar to a phase transition rather than a gradual deformation.

Formation of a black hole in a collision, which is then falling toward the AdS center, was first considered in [9], with a spherical black hole. Janik and Peschanski [10] proposed an asymptotic (late-time) solution, corresponding to rapidity-independent (Bjorken) flow; see [11,12] for the most recent advances along this direction.

Grumiller and Romatschke [13] tried to describe the initial stage of high energy collisions, starting with a certain type of gravitational shock waves. In Sec. V we will explore the formation of a horizon in a similar setup, but taking a different point of view: The image on the boundary must be due to the source in the bulk. This will lead to different and more consistent initial conditions, as well as subsequent evolution of matter.

A perturbative treatment of the initial conditions is discussed by Albacete, Kovchegov, and Taliotis [14]. Other models of equilibration based on solutions to dynamical Einstein equations include the model in our previous work [15], in which a gravitationally collapsing shell of matter in AdS_5 space is considered. This sheds light on how the formation of isotropic and homogeneous plasma may proceed through a very specific ''quasiequilibrium'' stage. We calculated the spectral densities and found that they deviate from their thermal counterpart by general oscillations. Another interesting solution describing isotropization of plasma was proposed by Chesler and Yaffe [16] recently.

The issue we will address in this work is the formation of trapped surfaces and entropy production in the collision of two shock waves in AdS background. Work in this direction in the AdS/CFT context started with the paper by Gubser, Pufu, and Yarom [17], who considered *central*

*slin@grad.physics.sunysb.edu
†shuryak@tonic.physics.sunysb.edu

collisions of pointlike black holes in the bulk. They located the (marginally) trapped surface at the collision moment. Its area was then used as an estimate (more accurately, the lower bound) of the entropy produced in the collision. In the limit of very large collision energy E, they found that the entropy grows as $E^{2/3}$. In Sec. VI we will critically discuss how realistic these results are.

In this work we extend the work of Ref. [17] in two directions. One is the extension to the collision of shock waves with a *nonzero* impact parameter. Like for shock wave collision in asymptotically flat Minkowski background [18–20], in AdS background there is also an interesting switching of description: Beyond a certain impact parameter, the trapped surface disappears and the black hole formation no longer happens. The other direction deals with a simpler case of the so-called wall-on-wall collision—the collision of objects with infinite extension in transverse coordinates and nontrivial dependence in the holographic direction only, which was, in a way, overlooked before.

II. GRAVITATIONAL COLLISIONS AND TRAPPED SURFACES

The AdS/CFT approach is a duality between the $\mathcal{N} = 4$ super Yang-Mills theory in $3 + 1$ dimensions and string theory in $AdS_5 \times S^5$ 10-D space-time. At a large number of colors string theory is in the classical (supergravity) regime. Here (and in many other related works) the angles of the sphere S^5 play no role. The five-dimensional AdS_5 space has the background metric, which we will write as

$$ds^2 = L^2 \frac{-dudv + (dx^1)^2 + (dx^2)^2 + dz^2}{z^2} \tag{1}$$

where $u = t - x^3$ and $v = t + x^3$. x^3 is the longitudinal coordinate and x^1, x^2 are transverse coordinates. The effective gravity in this space (the bulk) can be related, by certain rules, to the $z = 0$ 4-D boundary, where the gauge theory lives. The background metric corresponds to the vacuum state of the gauge theory.

The ultrarelativistic nucleus-nucleus collisions we want to model are described in the bulk as a collision of certain objects, whose holograms are the colliding nuclei. The first step of [17] was a suggestion to model the nuclei by bulk pointlike masses. (We will return to a critical discussion of this point at the end of the paper.) Their gravity field corresponds to that of small black holes, and after a Lorentz boost to high energy, their field becomes very thin gravitational shock waves. As the shock waves approach each other, they do not interact until they meet at the collision point, for causal reasons. Nevertheless, the trapped surfaces associated with each shock wave grow as they approach the collision point, and finally merge. Note that the causality is not violated by this behavior because the trapped surface is not a physical object: In a way, this tells us what happens *after* the collision occurs. The existence of a trapped surface signifies black hole formation, since the matter inside it would not be able to escape.

Although in this work we attempt to solve the Einstein equations for times after collision, let us, for completeness, mention what happens next. For central collisions (or noncentral ones with the impact parameter below the critical value) two colliding objects form one central black hole. Its Hawking temperature and Bekenstein entropy are perceived by the observers at the boundary $z = 0$ as the initial temperature and entropy produced in gauge theory. When produced, the horizon of this black hole is strongly deformed, but (due to its dissipative nature) it eventually settles down locally to some stationary black hole metric. This black hole is simultaneously falling toward the AdS center ($z \to \infty$): The hologram of this is the cooling and expansion of matter produced in a collision. Since the boundary theory is conformal and equally strongly interacting at all scales, such cooling and expansion of plasma continues to arbitrarily low temperatures.

The importance of the trapped surface is in its determination of what part of the system *must* end up inside the black hole. The part outside it may be carried away (as gravitational radiation) or still fall inward: Thus one gets only the lower bound of the black hole mass. In this paper, we will concentrate on locating the trapped surface at the collision point and use the area of the trapped surface as a lower bound on the final black hole entropy, which by AdS/CFT corresponds to the entropy production of nucleus collisions in gauge theory.

The gravitational shock waves used in [17] are written as

$$ds^2 = L^2 \frac{-dudv + (dx^1)^2 + (dx^2)^2 + dz^2}{z^2} + L \frac{\Phi(x^1, x^2, z)}{z} \delta(u) du^2 \tag{2}$$

with the transverse profile $\Phi(x^1, x^2, z)$ satisfying the equation

$$\left(\Box - \frac{3}{L^2}\right)\Phi = 16\pi G_5 J_{uu} \tag{3}$$

with some bulk source J_{uu}, an arbitrary function. The operator $\Box$ is the hyperbolic Laplacian on the space

$$ds^2_{H3} = L^2 \frac{(dx^1)^2 + (dx^2)^2 + dz^2}{z^2}. \tag{4}$$

The shock wave moving in the $-x^3$ direction can be obtained by the substitution $u \leftrightarrow v$ to (2) and (3).

The trapped surface is determined from the zero (nonpositivity) of the so-called *expansion* $\theta \le 0$, depending on the metric. For a detailed explanation of its geometric and physical meaning, see e.g. [21]: It roughly corresponds to the expansion or contraction of the area between two light rays (null geodesics) emitted at some small distance from each other in the same direction. Its equality to zero corresponds to the so-called marginally trapped surface:

These light rays neither converge nor diverge. The trapped surface is made up of two pieces: $\mathcal{S} = \mathcal{S}_1 \cup \mathcal{S}_2$. $\mathcal{S}_1(\mathcal{S}_2)$ is associated with a shock wave moving in the $+x^3(-x^3)$ direction before collision. An additional condition is that the outer null vector normal to $\mathcal{S}_1$ and $\mathcal{S}_2$ must be continuous at the intersection $\mathcal{C} = \mathcal{S}_1 \cap \mathcal{S}_2$ point $u = v = 0$ to avoid a delta function in the expansion.

To find the $\mathcal{S}_1$ associated with the first shock wave,

$$ds^2 = L^2 \frac{-dudv + (dx^1)^2 + (dx^2)^2 + dz^2}{z^2} + L\frac{\Phi_1(x^1, x^2, z)}{z}\delta(u)du^2, \tag{5}$$

the following coordinate transformation is made to eliminate the discontinuity in geodesics:

$$v \to v + \frac{z}{L}\Phi_1\Theta(u) \tag{6}$$

where $\Theta(u)$ is the Heaviside step function. $\mathcal{S}_1$ is parametrized by

$$u = 0, \qquad v = -\psi_1(x^1, x^2, z). \tag{7}$$

The expansion is defined by $\theta = h^{\mu\nu}\nabla_\mu l_\nu$, with l_ν the outer null vector normal to $\mathcal{S}_1$. $h^{\mu\nu}$ is the induced metric. It can be constructed from three spacelike unit vectors w_1^μ, w_2^μ, w_3^μ, which are normal to $\mathcal{S}_1$:

$$h^{\mu\nu} = w_1^\mu w_1^\nu + w_2^\mu w_2^\nu + w_3^\mu w_3^\nu. \tag{8}$$

The vanishing of the expansion corresponds to the following equation:

$$\left(\Box - \frac{3}{L^2}\right)(\Psi_1 - \Phi_1) = 0 \tag{9}$$

with $\Psi_1(x^1, x^2, z) = \frac{L}{z}\psi_1(x^1, x^2, z)$.

The vanishing of the expansion on $\mathcal{S}_2$ associated with the second shock wave can be worked out similarly:

$$\left(\Box - \frac{3}{L^2}\right)(\Psi_2 - \Phi_2) = 0. \tag{10}$$

At the intersection $\mathcal{C} = \mathcal{S}_1 \cap \mathcal{S}_2$, $\mathcal{S}_1$ and $\mathcal{S}_2$ coincide; therefore, $\Psi_1(x^1, x^2, z) = \Psi_2(x^1, x^2, z) = 0$. The continuity of the outer null normal can be guaranteed by $\nabla\Psi_1 \cdot \nabla\Psi_2 = 4$.

In summary, finding a marginally trapped surface becomes the following unusual boundary value problem:

$$\left(\Box - \frac{3}{L^2}\right)(\Psi_1 - \Phi_1) = 0, \qquad \left(\Box - \frac{3}{L^2}\right)(\Psi_2 - \Phi_2) = 0, \qquad \Psi_1|_{\mathcal{C}} = \Psi_2|_{\mathcal{C}} = 0. \tag{11}$$

The boundary $\mathcal{C}$ should be chosen to satisfy the constraint

$$\nabla\Psi_1 \cdot \nabla\Psi_2|_{\mathcal{C}} = 4. \tag{12}$$

Note that (11) and (12) are written in the form of a scalar equation, invariant under coordinate transformation. For central collision, the sources J_{uu} are identical for two shock waves. In [17], for simplicity, they are chosen to be point-like in the bulk,

$$J_{uu} = E\delta(u)\delta(z - L)\delta(x^1)\delta(x^2). \tag{13}$$

The solution of Φ corresponding to this source gives rise to the following stress tensor on the boundary field theory:

$$T_{uu} = \frac{L^2}{4\pi G_5}\lim_{z\to 0}\frac{\Phi(x^1, x^2, z)\delta(u)}{z^3} = \frac{2L^4 E}{\pi(L^2 + (x^1)^2 + (x^2)^2)^3}\delta(u). \tag{14}$$

The parameters E and L can be tuned according to the energy and the transverse size of the nucleus.

The special source (13) preserves an $O(3)$ symmetry in H_3, which is manifest in the following coordinate system:

$$ds^2_{H3} = \frac{dr^2}{1 + r^2/L^2} + r^2(d\theta^2 + \sin^2\theta d\phi^2) \tag{15}$$

with the point source sitting at $r = 0$. We will elaborate the symmetry later in the context of noncentral collision.

The $O(3)$ symmetry helps to solve (11) analytically. The area of the trapped surface can be calculated and can give a lower bound to the entropy produced in the collision of shock waves, assuming the area theorem holds in AdS background.

For noncentral collision, the situation is complicated by the loss of $O(3)$ symmetry. In Minkowski background, the problem of the noncentral collision of point shock waves in $D = 4$ was solved beautifully in [18] by conformal transformation. In $D > 4$, it was solved numerically in [19]. In all cases, a critical impact parameter was found, beyond which the trapped surface ceased to exist.

In the next section, we will cast (11) into an integral equation, which allows us to solve (11) numerically.

III. CALCULATION OF THE TRAPPED SURFACE

Note that (11) resembles the electrostatic problem in flat space, with Ψ being the electric potential. We are familiar with the fact that the electric potential can be expressed as an integral of surface charge density. We want to see if this can be achieved in AdS space.

Let us start with the electrostatic problem in flat space. Consider the following electrostatic problem, which is similar to (11):

$$\nabla^2\Psi_i(x) = \nabla^2\Phi_i(x), \tag{16}$$

$$\Psi_i(x)|_{\mathcal{C}} = 0, \tag{17}$$

$$\nabla\Psi_1 \cdot \nabla\Psi_2 = 4, \tag{18}$$

where $i = 1, 2$, and ∇^2 is the Laplacian in flat space. Ψ_i is the electric potential corresponding to the source $\nabla^2\Phi_i$,

placed inside an empty chamber with the conducting boundary $\mathcal{C}$. The boundary should be chosen properly such that the constraint (18) is also satisfied.

We want to express the electric potential by an integral of the surface charge density. This can be done with the help of the free boundary Green's function defined as the solution to

$$\nabla^2 G(x, x') = \delta^{(3)}(\vec{x} - \vec{x}'), \tag{19}$$

with the solution given by

$$G(x, x') = -\frac{1}{4\pi}\frac{1}{|\vec{x} - \vec{x}'|}. \tag{20}$$

Taking (16) multiplied by $G(x, x')$ minus (19) multiplied by $\Psi_i(x)$, and then integrating over the space inside $\mathcal{C}$, we obtain

$$\int d^3x (G(x, x')\nabla^2\Psi_i(x) - \Psi_i(x)\nabla^2 G(x, x')) = \int d^3x G(x, x')\nabla^2\Phi_i(x) - \Psi_i(x'), \tag{21}$$

$$\int d\vec{S}\cdot(G(x, x')\vec{\nabla}\Psi_i(x) - \Psi_i(x)\vec{\nabla}G(x, x')) = \int d^3x G(x, x')\nabla^2\Phi_i(x) - \Psi_i(x'). \tag{22}$$

Denote $B_i(x) = -\frac{\partial\Psi_i(x)}{\partial n}$ (the magnitude of the electric field on the boundary) and note that $\Psi_i(x)$ vanishes on the boundary. With x' taken on the boundary $\mathcal{C}$, (22) evaluates to

$$\int dS G(x, x')B_i(x) = \int d^3x G(x, x')\nabla^2\Phi_i(x). \tag{23}$$

The constraint (18) is simply $B_1(x)B_2(x) = 4$. We have converted a problem in the volume into a problem on its boundary $\mathcal{C}$. Equation (23) is a Fredholm integral equation of the first kind. We can use the following method to solve (16): Starting with some trial shape of $\mathcal{C}$, we can solve (22) to obtain $B_i(x)$ and check if (18) is satisfied. We can use iteration to tune the trial shape until (18) is satisfied.

Now we hope to apply a similar method to the problem of a trapped surface, the difference being that the space is H_3 instead of flat.

As in the case of the electrostatic problem, we will keep using the Green's function in AdS, defined as the solution to the following:

$$\left(\Box - \frac{3}{L^2}\right)G(x, x') = \frac{1}{\sqrt{g}}\delta^{(3)}(\vec{x} - \vec{x}') \tag{24}$$

where g is the metric of H_3.

The Green's function was solved in [22,23]. We quote the result here with L dependence restored.

$$G(x, x') = -\frac{1}{4\pi L}\frac{e^{2u}}{\sinh u}, \qquad \cosh u = 1 + \frac{(z - z')^2 + (\vec{x}_\perp - \vec{x}'_\perp)^2}{2zz'}, \tag{25}$$

where u is the invariant distance in $H_3(\mathrm{AdS}_3)$.

It also proves useful to note another relation:

$$\int_M \Box f\sqrt{g}d^3x = \int_M \frac{1}{\sqrt{g}}\partial_\mu(\sqrt{g}g^{\mu\nu}\partial_\nu f)\sqrt{g}\frac{1}{3!}\epsilon_{\sigma\rho\lambda}dx^\sigma \wedge dx^\rho \wedge dx^\lambda = \int_M d\left(\sqrt{g}g^{\mu\nu}\partial_\nu f\epsilon_{\mu\rho\lambda}\frac{1}{2!}dx^\rho \wedge dx^\lambda\right) \tag{26}$$

where $\overline{dx}^\nu = g^{\mu\nu}\sqrt{g}\epsilon_{\mu\rho\lambda}\frac{1}{2!}dx^\rho \wedge dx^\lambda$. M is taken to be the manifold in H_3 bounded by $\mathcal{C}$, and the metric g refers to H_3. f is an arbitrary function of x.

With (25) and (26) at hand, we are ready to proceed:

$$\left(\Box - \frac{3}{L^2}\right)\Psi_i(x) = \left(\Box - \frac{3}{L^2}\right)\Phi_i(x), \qquad \left(\Box - \frac{3}{L^2}\right)G(x, x') = \frac{1}{\sqrt{g}}\delta^{(3)}(\vec{x} - \vec{x}'), \tag{27}$$

with $i = 1, 2$. All the derivatives are with respect to x. Taking the first line of (27) multiplied by $G(x, x')$ minus the second line of (27) multiplied by $\Psi_i(x)$, then integrating over M, we obtain

$$\int_M \left(G(x, x')\left(\Box - \frac{3}{L^2}\right)\Psi_i(x) - \Psi_i(x)\left(\Box - \frac{3}{L^2}\right)G(x, x')\right)\times\sqrt{g}d^3x = \int_M G(x, x')\left(\Box - \frac{3}{L^2}\right)\Phi_i(x)\sqrt{g}d^3x - \Psi_i(x'), \tag{28}$$

$$\int_M (G(x, x')d(\partial_\nu\Psi_i(x)\overline{dx}^\nu) - \Psi_i(x)d(\partial_\nu G(x, x')\overline{dx}^\nu)) = \int_M G(x, x')\left(\Box - \frac{3}{L^2}\right)\Phi_i(x)\sqrt{g}d^3x - \Psi_i(x'), \tag{29}$$

$$\int_M (d(G(x, x')\partial_\nu\Psi_i(x)\overline{dx}^\nu) - d(\Psi_i(x)\partial_\nu G(x, x')\overline{dx}^\nu)) = \int_M G(x, x')\left(\Box - \frac{3}{L^2}\right)\Phi_i(x)\sqrt{g}d^3x - \Psi_i(x'), \tag{30}$$

$$\int_{\partial M} (G(x, x')\partial_\nu\Psi_i(x)\overline{dx}^\nu - \Psi_i(x)\partial_\nu G(x, x')\overline{dx}^\nu) = \int_M G(x, x')\left(\Box - \frac{3}{L^2}\right)\Phi_i(x)\sqrt{g}d^3x - \Psi_i(x'), \tag{31}$$

where in the last line we have used Stokes theorem on manifold M.

Putting x' on $\mathcal{C}$, we can simplify the above with $\Psi_i|_{\mathcal{C}} = 0$:

$$\int_{\partial M} G(x,x')\partial_\nu \Psi_i(x)\overline{dx}^\nu = \int_M G(x,x')\left(\Box - \frac{3}{L^2}\right)\Phi_i(x)\sqrt{g}d^3x. \tag{32}$$

Furthermore, we have $\partial_\nu \psi dx^\nu = 0$ on $\mathcal{C}$ since $\Psi_i|_{\mathcal{C}} = 0$. On the other hand, $n_\nu dx^\nu|_{\mathcal{C}} = 0$, where n_ν is the unit vector normal to the boundary $\mathcal{C}$. Therefore, we may write

$$\partial_\nu \Psi_i = -B_i n_\nu. \tag{33}$$

Equations (12) and (32) can be further simplified with (33):

$$-\int_{\partial M} G(x,x')B_i(x)dS = \int_M G(x,x')\left(\Box - \frac{3}{L^2}\right)\Phi_i(x)\sqrt{g}d^3x, \tag{34}$$

$$B_1(x)B_2(x) = 4, \tag{35}$$

where $dS \equiv n_\mu \overline{dx}^\mu$ is the area element.

Before proceeding to noncentral collision, we would like to reproduce the 5-D result of [17] first. Working in spherical coordinates (15), the shape of $\mathcal{C}$ is parametrized by $r = \rho_0 = \text{const}$. The simplest point shock wave corresponding to $J_{uu} = E\delta(u)\delta(z-L)\delta(x^1)\delta(x^2)$ is given by

$$\Phi_1 = \Phi_2 = \frac{4G_5E}{L}\frac{1 + 2(r/L)^2 - 2r/L\sqrt{1+(r/L)^2}}{r/L}. \tag{36}$$

The Green's function (25) is invariant under coordinate transformation. In spherical coordinates, it is given by

$$G(x,x') = -\frac{1}{4\pi L}\frac{e^{2u}}{\sinh u},$$
$$\cosh u = \sqrt{r^2/L^2+1}\sqrt{r'^2/L^2+1} - rr'/L^2(\cos\theta\cos\theta' + \sin\theta\sin\theta'\cos(\phi-\phi')). \tag{37}$$

In the presence of $O(3)$ symmetry, it is sufficient to show that (34) holds for $\theta' = 0$, when the integral in ϕ is trivial. On the other hand, (35) implies $B_1 = B_2 = 2$. As a result, we only need to verify

$$2\pi\int_0^\pi d\theta(-2)\frac{(\cosh u - \sinh u)^2}{\sinh u}\rho_0^2\sin\theta = \frac{(\sqrt{\rho_0^2+1}-\rho_0)^2}{\rho_0}(-4G_5E)4\pi\cosh u = \rho_0^2 + 1 - \rho_0^2\cos\theta. \tag{38}$$

It is not difficult to complete the integral in θ; we finally arrive at $2G_5E = \sqrt{1+\rho_0^2/L^2}\rho_0^2$, which is equivalent to (115) in [17].

IV. COLLIDING POINT SHOCK WAVES AT A NONZERO IMPACT PARAMETER

A. Shock waves in spherical coordinates

Consider two shock waves with impact parameter b, given by

$$\left(\Box - \frac{3}{L^2}\right)\Psi_1 = -16\pi G_5 E\delta(u)\delta(z-z_0)\delta\left(x^1 - \frac{b}{2}\right)\delta(x^2),$$
$$\left(\Box - \frac{3}{L^2}\right)\Psi_2 = -16\pi G_5 E\delta(u)\delta(z-z_0)\delta\left(x^1 + \frac{b}{2}\right)\delta(x^2). \tag{39}$$

The corresponding stress energy tensors associated with two shock waves are given by

$$T_{uu} = \frac{2L^4E}{\pi(z_0^2 + (x^1 - \frac{b}{2})^2 + (x^2)^2)^3}\delta(u),$$
$$T_{vv} = \frac{2L^4E}{\pi(z_0^2 + (x^1 + \frac{b}{2})^2 + (x^2)^2)^3}\delta(v).$$

Therefore, z_0 characterizes the size of the nucleus. We will use spherical coordinates in solving (34). In the case of central collision, when $b = 0$, the shock wave center can be placed at the origin of spherical coordinates $r = 0$. This is achieved by first going to global coordinates $Y^i (i = 0, 1, 2, 3)$:

$$Y^0 = \frac{z}{2}\left(k + \frac{L^2/k + kx_\perp^2}{z^2}\right),$$
$$Y^3 = \frac{z}{2}\left(-k + \frac{L^2/k - kx_\perp^2}{z^2}\right),$$
$$Y^1 = L\frac{x^1}{z}, \qquad Y^2 = L\frac{x^2}{z}. \tag{40}$$

The global coordinates are linked to spherical coordinates in the following way:

$$Y^0 = \sqrt{r^2+L^2}, \qquad Y^1 = r\cos\theta,$$
$$Y^2 = r\sin\theta\cos\phi, \qquad Y^3 = r\sin\theta\sin\phi. \tag{41}$$

When $b = 0$, the center of the shock waves can be put at the origin if we set $k = \frac{L}{z_0}$. The possibility of moving any point to the origin reflects the maximally symmetric property of AdS space.

When $b \neq 0$, we want to place the two shock waves at opposite positions with respect to the origin, so that the boundary of the trapped surface $\mathcal{C}$ will have axial symmetry. Setting $1 + \frac{b^2}{4z_0^2} = \frac{L^2}{k^2 z_0^2}$, we have $Y^2 = Y^3 = 0$ and $Y^1 = \pm\frac{Lb}{2z_0}$. According to (41), we have the shock waves at

$r = \frac{Lb}{2z_0}$, $\theta = 0$, and $\theta = \pi$. The differential equation in (34) becomes

$$\left(\Box - \frac{3}{L^2}\right)\Psi_i = -16\pi G_5 E \frac{L^3}{z_0^3} \frac{\sqrt{1 + r^2/L^2}}{r^2 \sin\theta} \delta(r - r_0) \times \delta(\theta - \theta_i)\delta(\phi) \tag{42}$$

where $r_0 = \frac{Lb}{2z_0}$, $\theta_1 = 0$, $\theta_2 = \pi$. We observe that, in spherical coordinates, the trapped surface only depends on $G_5 E \frac{L^3}{z_0^3}$ and r_0. Since the AdS radius is a free parameter, which will not appear alone in the final result in dual field theory, we may set $z_0 = L$ without loss of generality. As a result we have $b = 2r_0$.

B. More general shock waves

Before proceeding to the numerical study of trapped surfaces, we choose to take a moment to investigate the symmetries of the problem, which will help us to study more general shock waves. To see this, we prefer to work in the differential form of the problem: (11) and (12).

As we noticed before, (11) and (12) are scalar equations. Ψ_i is a scalar. It is invariant under coordinate transformations: $x \to \tilde{x}$, $\Psi_i(x) \to \tilde{\Psi}_i(\tilde{x})$. The boundary remains the same $\mathcal{C} \to \tilde{\mathcal{C}}$, but takes a different functional form in new coordinate. As a result, (12) is automatically satisfied. Suppose the transformation also preserves the form of the operator: $\Box - 3/L^2$, then $\tilde{\Psi}_i(\tilde{x})$ becomes another solution to (11) and (12). We will focus on transformations that leave the center of the shock waves on the axis of $\theta = 0, \pi$.

To identify such a coordinate transformation, we first make a change of variables:

$$r\sin\theta = t, \qquad r\cos\theta = \sqrt{L^2 + t^2}\sinh\eta.$$

The metric of H_3 becomes

$$ds^2 = \frac{dt^2}{1 + t^2/L^2} + (L^2 + t^2)d\eta^2 + t^2 d\phi^2. \tag{43}$$

The metric is η independent; therefore the transformation $\tilde{t} = t$, $\tilde{\phi} = \phi$, $\tilde{\eta} = \eta + \Delta\eta$ will not change the operator $\Box - 3/L^2$. $\tilde{t} = t$ also guarantees that the center of the shock waves remains on the axis of $\theta = 0, \pi$. We have obtained the desired coordinate transformation, which is just a translation in η. It is easy to work out the corresponding transformation in spherical coordinates:

$$\begin{aligned} \tilde{r}\sin\tilde{\theta} &= r\sin\theta = t, \\ \tilde{r}\cos\tilde{\theta} &= \sqrt{L^2 + t^2}\sinh(\eta - \Delta\eta), \\ r\cos\theta &= \sqrt{L^2 + t^2}\sinh\eta. \end{aligned} \tag{44}$$

One can verify explicitly that (44) preserves the form of (15). Equation (44) moves the center of the shock waves from $Y^2 = Y^3 = 0$, $Y^1 = \pm r_0$ to $Y^2 = Y^3 = 0$, $Y^1 = \pm r_0\cosh\Delta\eta - \sqrt{L^2 + r_0^2}\sinh\Delta\eta$. This means that the collision of shock waves centered at $Y^2 = Y^3 = 0$, $Y^1 = \pm r_0\cosh\Delta\eta - \sqrt{L^2 + r_0^2}\sinh\Delta\eta$ will generate the same entropy as those centered at $Y^2 = Y^3 = 0$, $Y^1 = \pm r_0$. This allows us to study the collision of more general shock waves. Let us consider the following shock waves:

$$\begin{aligned} \left(\Box - \frac{3}{L^2}\right)\Psi_1 &= -16\pi G_5 E_u \delta(u)\delta(z - z_u)\delta(x^1 - x_u)\delta(x^2), \\ \left(\Box - \frac{3}{L^2}\right)\Psi_2 &= -16\pi G_5 E_v \delta(v)\delta(z - z_v)\delta(x^1 - x_v)\delta(x^2). \end{aligned} \tag{45}$$

In this paper, we restrict our interest to shock waves with identical invariant energy, defined by $E_u \frac{L^3}{z_u^3} = E_v \frac{L^3}{z_v^3} \equiv E$. This keeps the mirror symmetry of the problem intact. We will see that the center of the shock waves can be placed at

$$Y^2 = Y^3 = 0, \qquad Y^1 = \pm r_0\cosh\Delta\eta - \sqrt{L^2 + r_0^2}\sinh\Delta\eta.$$

This is equivalent to the statement that a solution to the following equations can always be found:

$$\begin{aligned} L\frac{x_u}{z_u} &= r_0\cosh\Delta\eta - \sqrt{L^2 + r_0^2}\sinh\Delta\eta, \\ L\frac{x_v}{z_v} &= -r_0\cosh\Delta\eta - \sqrt{L^2 + r_0^2}\sinh\Delta\eta, \\ k^2\left(1 + \frac{x_u^2}{z_u^2}\right) &= \frac{L^2}{z_u^2}, \qquad k^2\left(1 + \frac{x_v^2}{z_v^2}\right) = \frac{L^2}{z_v^2}, \\ x_u - x_v &= \Delta x. \end{aligned} \tag{46}$$

Equation (46) can be solved easily by switching to the variable $\eta_0 = \sinh^{-1}\frac{r_0}{L}$. A solution to (46) always exists for any given z_u, z_v, and Δx. We include the corresponding r_0 here, as it is the only relevant quantity, apart from E, for entropy calculation:

$$\frac{r_0}{L} = \sqrt{\frac{(z_u - z_v)^2 + \Delta x^2}{4z_u z_v}}. \tag{47}$$

In summary, we have shown that for shock waves (45) satisfying $E_u \frac{L^3}{z_u^3} = E_v \frac{L^3}{z_v^3} \equiv E$, the entropy is only a function of $G_5 E$ and (47). Note that r_0 is only a function of the invariant distance between the centers of the shock waves.

C. Numerical solution of trapped surfaces

With all the simplification, we are ready to find the trapped surface for different impact parameters. Our procedure is as follows: Axial symmetry allows us to parametrize $\mathcal{C}$ by $r = \rho(\theta)$. Integrals in ϕ on the left-hand side of (34) can be expressed in terms of elliptic integrals. Equation (34) becomes essentially a 1-D integral equation.

We discretize the integral by 199 points, equally spaced in the full range of θ. The integral on the left-hand side of (34) is discretized accordingly, and the integral on the right-hand side can be expressed in terms of an elementary function due to the simple form of the shock wave. We use the same sample points for θ', bringing (34) into a matrix form:

$$\sum_j B(\theta_j)K(\theta_j, \theta_i') = S(\theta_i') \tag{48}$$

where the indices $i, j = 1, \ldots, 199$. $K(\theta_j, \theta_i')$ contains the Green's function and the induced metric. $S(\theta_i')$ is from the right-hand-side integral of the shock wave.

A special treatment is needed for the diagonal matrix element of $K(\theta_j, \theta_i')$, where $\theta_j = \theta_i'$. The explicit integrand expressed in terms of elliptic integrals shows that it is logarithmically divergent in $|\theta - \theta'|$, yet the integral is convergent. The integral in this interval, represented by the diagonal matrix element, is estimated by sampling the integrand by a certain number of points in the interval. The sample integrand is used to extract the coefficients of the terms $\ln|\theta - \theta'|$, 1, $(\theta - \theta')\ln|\theta - \theta'|$, and $\theta - \theta'$ by the method of least squares. Those coefficients are finally used for the calculation of diagonal matrix elements.

The mirror symmetry of the two shock waves implies $B_2(\theta) = B_1(\pi - \theta)$. Therefore, it is sufficient to calculate one of them. Given a trial shape of the trapped surface $r = \rho(\theta)$, which is also necessarily symmetric under $\theta \leftrightarrow \pi - \theta$, we can solve for $B(\theta)$ from (48). We then evaluate $\Delta(\theta) = B_1(\theta)B_2(\theta) - 4$ and tune the shape function accordingly. We repeat the process until (35) is satisfied to a certain accuracy. In order to assure fast convergence, we find it very helpful to calculate the gradient of $\rho(\theta)$. The gradient is the matrix form of the functional derivative: $\frac{\delta\Delta[\rho(\theta)]}{\delta\rho(\theta)}$. We parametrized $\mathcal{C}$ by $\rho(\theta) = \sum_{n=1}^{M} a_n \cos 2(n-1)\theta$, where M is a truncation number. The same decomposition applies to $\Delta(\theta)$: $\Delta(\theta) = \sum_{n=1}^{M} b_n \cos 2(n-1)\theta$. The gradient in this representation is given by an $M \times M$ matrix: $\frac{\delta b_m}{\delta a_n}$, which again contains elliptic integrals. For a given collision energy, we can find the boundary $\mathcal{C}$ until a certain critical impact parameter is reached. The critical impact parameter is located where $\frac{\partial\rho(\theta)}{\partial b}$ diverges [19]. Empirically, the gradient $\frac{\delta b_m}{\delta a_n}$ converges as $\Delta(\theta)$ reduces in the iteration, if the impact parameter is within the critical value. The gradient diverges as $\Delta(\theta)$ is reduced in the iteration, if the impact parameter lies beyond the critical value.

Figure 1 shows the shapes of the trapped surfaces at $\frac{G_5 E}{L^2} = 1$ and $\frac{G_5 E}{L^2} = 100$ for different impact parameters. The shapes are represented in spherical coordinates. We observe that the critical trapped surface does not scale with collision energy in spherical coordinates. As collision energy grows, the trapped surface gets elongated in the axis of mismatch and larger M is needed to reach the prescribed accuracy.

We also obtained several critical impact parameters corresponding to different energies. The results are listed in Table. I.

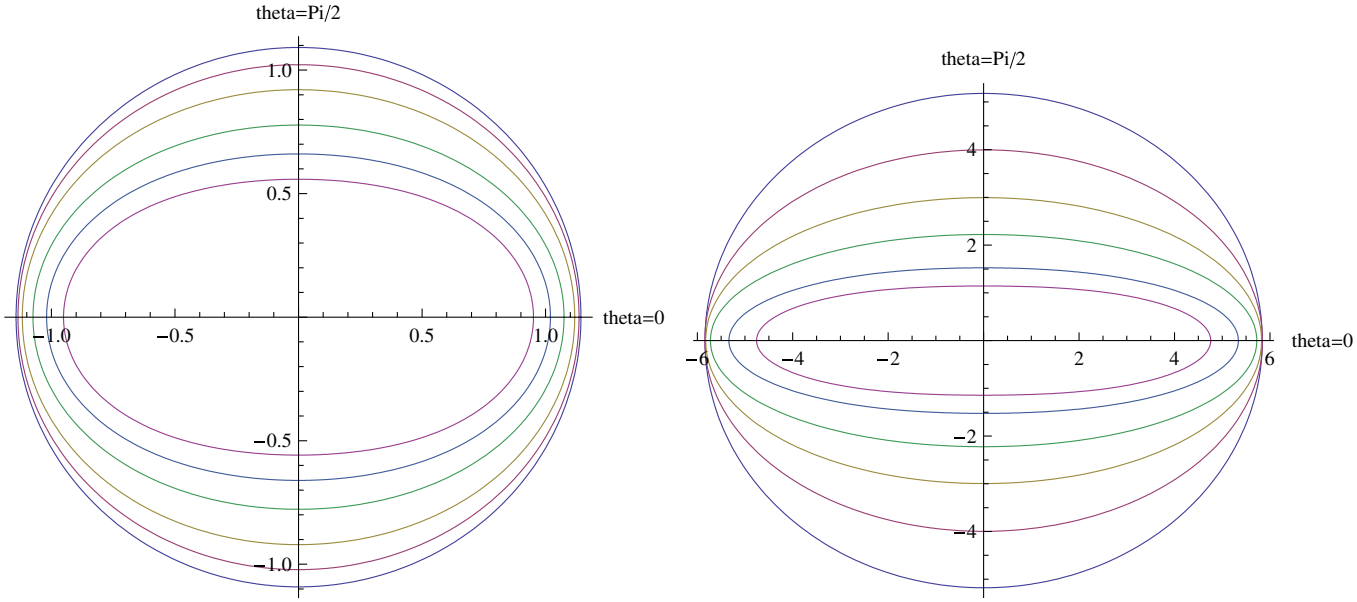

FIG. 1 (color online). Left panel: The shapes of $\mathcal{C}$ (the trapped surface at $u = v = 0$) at $\frac{G_5 E}{L^2} = 1$. The impact parameters used in the plot are $0.4L$, $0.6L$, $0.8L$, $1.0L$, $1.1L$, $1.14L$, from outside to inside, the innermost shape being the critical trapped surface. Right panel: The shapes of $\mathcal{C}$ (the trapped surface at $u = v = 0$) at $\frac{G_5 E}{L^2} = 100$. The impact parameters used in the plot are $1.0L$, $2.0L$, $3.0L$, $4.0L$, $5.0L$, $5.3L$, from outside to inside, the innermost shape being the critical trapped surface. As collision energy grows, the trapped surface gets elongated in the axis of mismatch.

TABLE I. Critical impact parameter at different energies.

$\frac{G_5E}{L^2}$	0.1	0.5	1	4	9	12	15	50	100
$\frac{b_c}{L}$	0.40	0.86	1.14	1.90	2.50	2.74	2.94	4.28	5.30

Figure 2 shows the log-log plot of the critical impact parameter versus collision energy. It suggests a simple power law within the energy range used in the numerical study. The data are fitted with $\frac{b_c}{L} = \alpha(\frac{G_5E}{L^2})^\beta$ to give

$$\alpha = 1.07, \qquad \beta = 0.37. \tag{49}$$

$b \sim E^\beta L^{1-2\beta}$, the numerical value from fitting, shows that the critical impact parameter grows with collision energy and nucleus size.

The area of the trapped surface (twice the area of $\mathcal{C}$) sets a lower bound of the entropy produced, which is given as follows:

$$S_{\text{trapped}} = \frac{2A}{4G_5} = \frac{1}{2G_5}\int \sqrt{g}d^3x \tag{50}$$

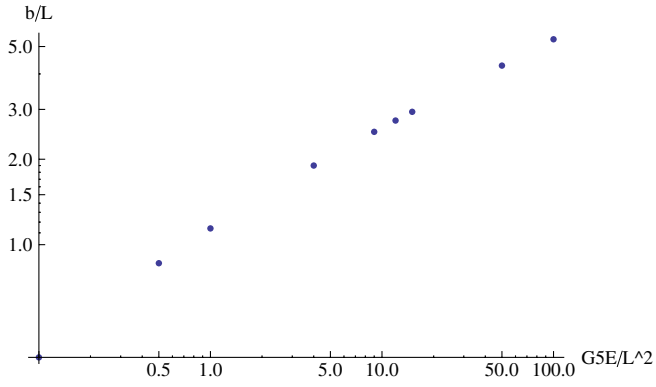

FIG. 2 (color online). The log-log plot of the critical impact parameter versus collision energy.

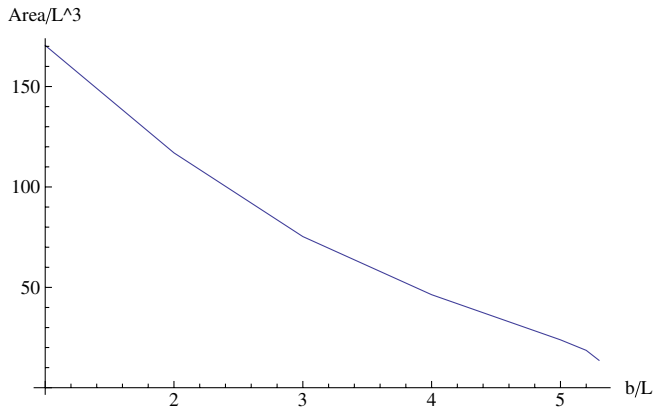

FIG. 3 (color online). The scaled entropy $2G_5S/L^3$ (the area of $\mathcal{C}$) as a function of the scaled impact parameter b/L. The energy used is $\frac{G_5E}{L^2} = 100$, where $\frac{L^3}{G_5} = \frac{2N_c^2}{\pi}$.

where A is the area of the boundary $\mathcal{C}$. The prefactor is

$$\frac{L^3}{G_5} = \frac{2N_c^2}{\pi}. \tag{51}$$

We plot the lower bound of the entropy in the dual field theory for energy $\frac{G_5E}{L^2} = 100$ in Fig. 3.

V. WALL-ON-WALL COLLISIONS

In this section we address a simpler form of the shock waves (called wall-on-wall in [9]), in which there is no dependence on two transverse coordinates. Grumiller and Romatschke [13] have also discussed it, using gravitational shock waves. The problem with their approach is the (power) growing amplitude of the shock as a function of holographic coordinate z. Thus, collision dynamics resembles the atmospheric turbulence in the sense that the largest perturbation is at the largest z—namely, in the infrared modes—cascading down toward higher momenta (UV). First of all, this is physically different from the heavy ion collisions, in which case the initial wave functions have partons well localized near the so-called "saturation scale," from which the equilibration domain (trapped surface) propagates both into small z (UV) and large z (IR) directions. Second, we think it is also inconsistent: A function growing with z cannot be considered as a small perturbation to the background metric, which is decreasing at large z as $1/z^2$. One may think that gravity near the AdS center $z = \infty$ should never be touched, as this is the original position of the D_3-branes which gave the basis for AdS/CFT correspondence in the first place.

Our choice of initial conditions, describing colliding walls with fixed parton density and thus a fixed saturation scale, is given by the following source:

$$\left(\Box - \frac{3}{L^2}\right)\Phi(z) = -16\pi\frac{G_5E}{L^2}\delta(z - z_0). \tag{52}$$

The corresponding solution to the Einstein equation, subject to the boundary condition $\Psi(z) \to 0$ as $z \to 0$, is easily obtained:

$$\Phi(z) = \begin{cases} 4\pi G_5 E\frac{z^3}{z_0^4} & z < z_0 \\ 4\pi G_5 E\frac{1}{z} & z > z_0. \end{cases} \tag{53}$$

Note that it decreases in both directions from the original scale z_0; therefore (as we will see shortly), the trapped surface has finite extensions in both directions.

The corresponding stress energy tensor on the boundary (as seen by an observer living in dual gauge theory) is

$$T_{uu} = \frac{EL^2}{z_0^4}\delta(u). \tag{54}$$

The stress energy tensor is the same as that used in [13,14], and our solution converges well as $z \to \infty$. We choose to collide states with different energy; therefore, we fix z_0, but

use different E. Applying the general discussion of shock waves in Sec. II and noting that the trapped surface only depends on z, we obtain

$$z^2\Psi_i'' - z\Psi_i' - 3\Psi_i = -16\pi G_5 E_i \delta(z - z_0), \tag{55}$$

$$\Psi_i(z_a) = \Psi_i(z_b) = 0, \tag{56}$$

with $i = 1, 2$. Ψ_1 and Ψ_2 are shape functions corresponding to two shock waves. The trapped region at $u = v = 0$ is limited by the interval $z_a < z < z_b$. The constraint (35) takes a simple form:

$$\Psi_1(z_a)\Psi_2(z_a)\frac{z_a^2}{L^2} = 4, \qquad \Psi_1(z_b)\Psi_2(z_b)\frac{z_b^2}{L^2} = 4. \tag{57}$$

Equation (55) is easily solved to give

$$\begin{aligned}\Psi_i(z) &= \begin{cases} C((\frac{z}{z_a})^3 - \frac{z_a}{z}) & z < z_0 \\ D((\frac{z}{z_b})^3 - \frac{z_b}{z}) & z > z_0, \end{cases} \\ C &= -4\pi G_5 E_i \frac{(\frac{z_0}{z_b})^3 - \frac{z_b}{z_0}}{(\frac{z_0}{z_a})^3 z_b - (\frac{z_0}{z_b})^3 z_a}, \\ D &= -4\pi G_5 E_i \frac{(\frac{z_0}{z_a})^3 - \frac{z_a}{z_0}}{(\frac{z_0}{z_a})^3 z_b - (\frac{z_0}{z_b})^3 z_a}. \end{aligned} \tag{58}$$

Plugging (58) into (57), we obtain

$$z_a + z_b = \frac{8\pi G_5\sqrt{E_1 E_2}}{L}, \tag{59}$$

$$\frac{(z_a + z_b)^2 - 3z_a z_b}{(z_a z_b)^3} = \frac{L^3}{z_0^4}. \tag{60}$$

Note that E_1, E_2 appear only in the combination $\sqrt{E_1 E_2}$. This is consistent with the picture that only the center of mass contributes to the entropy. Recall that the center of mass of two massless particles with energy E_1, E_2 is $2\sqrt{E_1 E_2}$. The resulting cubic equation (60) can be solved by the Cardano formula, but the explicit solution is not illustrative and is not shown here. The entropy is given by

$$\begin{aligned} S &= \frac{2A}{4G_5} = \frac{\int \sqrt{g} dz d^2x_\perp}{2G_5}, \\ s &\equiv \frac{S}{\int d^2x_\perp} = \frac{L^3}{4G_5}\left(\frac{1}{z_a^2} - \frac{1}{z_b^2}\right). \end{aligned} \tag{61}$$

The leading behavior of the entropy per transverse area s in energy is extracted:

$$s \sim \frac{4L^2}{z_0^4}(\pi G_5\sqrt{E_1 E_2} z_0^2)^{2/3}. \tag{62}$$

The power $2/3$ is the same as the point shock wave obtained in [17]. There is also an obvious lower bound of the energy for the formation of the trapped surface:

$$4\pi G_5 E \geq z_0. \tag{63}$$

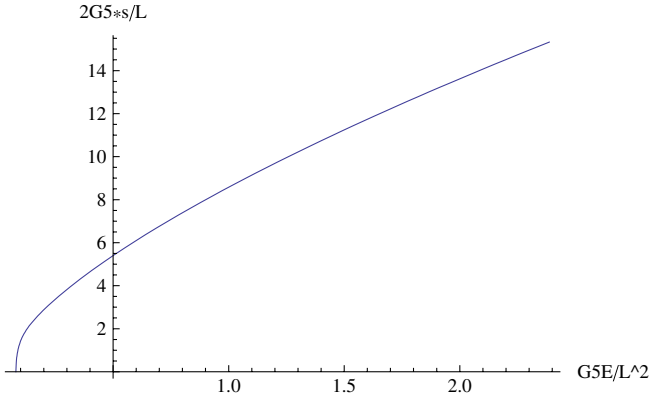

FIG. 4 (color online). The scaled entropy per transverse area $\frac{2G_5 s}{L^2}$ (the area of $\mathcal{C}$ per transverse area) as a function of scaled effective colliding energy $G_5 E/L^2$, where $\frac{L^3}{G_5} = \frac{2N_c^2}{\pi}$.

The equality is reached at $z_a = z_b$, when the $\mathcal{C}$ has vanishing volume. For general energy, s is evaluated as a function of effective colliding energy $E = \sqrt{E_1 E_2}$. We again set $z_0 = L$. Figure 4 shows the entropy as a function of effective colliding energy.

VI. MATCHING GRAVITATIONAL AND HEAVY ION COLLISIONS

So far, this has been a purely theoretical work devoted to solving well-posed mathematical problems, defined in terms of (the AdS/CFT dual) gravity framework. Now, near the end of this work, we would like to address wider issues of the limitations of such an approach, as well as the best strategies to put it to practical use.

Gubser *et al.* [17] have applied the gravitational collision scenario literally, selecting initial conditions at times long before nuclei collide. More specifically, they have (i) tuned the scale L or z_0 of the bulk colliding object to the size of the nucleus R and (ii) used the realistic center-of-mass gamma factor of the colliding nuclei $E/m = \gamma \sim 100$. The result of such a choice is a *rather unrealistic* fireball, in spite of a reasonable entropy. Indeed, the size of the trapped surface [17] is huge, about 30 fm, which is very large compared to colliding nuclei. In real heavy ion collisions the produced fireball has the same size as the nuclei, with a radius of about 6 fm. The initial temperature—as estimated by $z_{\min} \sim 1/\pi T_i$, where $z_{\min}$ is the minimal distance of the trapped surface to the AdS boundary—is, however, way too high. So, what can be wrong with this approach?

The answer to this question is, in fact, well known: The initial formation of the partonic wave function, describing nuclei at the collision moment, *cannot* be adequately described by the dual gravity. We know from experiment that growing partonic density makes hadrons and nuclei blacker and of larger size, as the collision energy grows. This is phenomenologically described by a Pomeron, a

power fitting to rising cross section $\sim s^{\alpha(t)-1}$. Although qualitatively similar to what happens in gravitational collisions, this growth is very different compared to that predicted in dual gravity. Indeed, the observed Pomeron intercept $\alpha(t=0)-1$–0.1, while in the AdS/CFT world the Pomeron intercept $\alpha(t=0)-1=1$ [24]. Thus the effective size of objects in gravitational collision grows with energy with an exponent 10 times that in real QCD. In view of this, one should clearly give up the idea of tuning the scale L or z_0 of the bulk colliding object to the size of the nucleus, and tune it perhaps to the parton density (''saturation scale'' Q_s in the ''color glass'' models) of the corresponding nuclear wave function.

More generally, we are dealing with a complicated problem in QCD, in which the effective coupling runs, from high to low scales as the collisions progress from an initial violent partonic stage toward equilibration, expansion, and cooling. So, in principle, it would be logical to switch—as smoothly as possible—from the weak-coupling based methods (such as classical Yang-Mills) to strong-coupling ones (such as AdS/CFT) at a certain proper time $\tau_{\rm switch}$ appropriately chosen by the evolution of the coupling.[1]

Therefore, one should not try to tune the parameters of the gravitational collision model to initial nuclei, at $\tau=-\infty$, or to ''decoherent'' partons at the collision moment, at $\tau=0$, but rather at the later time $\tau_{\rm switch}$.[2] Although at the moment we do not understand the evolution of the appropriate coupling quantitatively enough, one may always treat it as a parameter. The practical utility of the AdS/CFT approach at later times, $\tau>\tau_{\rm switch}$, still remains significant: Namely, one can use a much more fundamental dual gravity description instead of its near-equilibrium approximation, the hydrodynamics, currently used.

VII. ARE THERE CRITICAL IMPACT PARAMETERS IN HEAVY ION COLLISIONS?

Summarizing our findings in one sentence, there exists a discontinuity in grazing gravitational collisions in the AdS space. As one smoothly increases the impact parameter b, the trapped surface and black hole formation disappear suddenly, at a certain critical impact parameter $b_c(E)$ depending on the collision energy E. The reason for this seems quite general: By increasing b, one increases the angular momentum of the system while at the same time *decreasing* the mass which can be stopped, and at some moment—as one knows from the Kerr solution for rotating black holes—black hole formation becomes impossible.

Suppose the AdS gravitational shock waves can describe the strongly coupled plasma in heavy ion collisions; then one would expect similar behavior in heavy ion experiments. We have looked at the data and found that indeed there are experimental indications that a relatively rapid switch of the underlying dynamics at some $b_c(E)$ seems to exist.

The most straightforward observable is entropy, which is related to the particle multiplicity versus the impact parameter. In Fig. 5 (left panel) from [28] we show some data plotted as a function of the number of participants $N_{\rm part}$. The right side of the figure corresponds to all nucleons participating, or central collisions; toward the left side are peripheral collisions. There are indeed two values of multiplicity per participant observed, one for small systems, pp and dAu collisions (stars and crosses), and one for ''large'' systems, CuCu and AuAu (circles and squares). There must be a transition between them somewhere, but, unfortunately, the experimental multiplicity measurements for ''grazing'' collisions are not available yet.[3] So, unfortunately, we do not yet know how exactly the transition from one regime to another happens; nor do we know what $b_c(E)$ is, if it can be defined.

However, some other observables associated with the collective flows of excited matter do show rapid changes at certain $b_c(E)$. Some evidence for this was seen in the elliptic flow measurements, as deviations from the hydrodynamical predictions for peripheral collisions. These are seen even more clearly in the centrality dependence of the so-called ''ridge'' phenomenon (see its relation to flow in [29,30]), which we show in Fig. 5 (right panel).

Admittedly, these rapid changes in the dynamics have not been systematically studied yet, neither experimentally nor theoretically. The naive explanation often attributes the changes to the fact that they happen when the overlap system gets ''too small'' in terms of participating nucleons N_p, causing large enough fluctuations $O(1/\sqrt{N_p})$. However, if this were the reason, one would expect this jump to be dependent on N_p and *not* dependent on the collision energy. Furthermore, the gravitational collisions do not have any discrete elements at all, while predicting $b_c(E)$ growing with E, as observed in Fig. 5. We therefore suggest that angular momentum may also be important; this issue clearly deserves to be studied further.

VIII. CONCLUSIONS

In this work we have developed a method to solve for the shape of the trapped surface based on an analogy to the electrostatic problem in flat space: The main idea is to proceed from the differential to the integral form of the equation. We used this method to obtain the shape of

[1]The so-called AdS/QCD approach (see e.g. [25,26]) tries to incorporate the running coupling into the gravitational framework. A particularly simple example of this is a jump of the coupling at a certain ''domain wall'' scale proposed in [27].

[2]It is proposed in [14] that one may choose to collide some special unphysical shock waves.

[3]Small multiplicity collisions are detected for all systems, but their accurate separation from beam-residual gas collisions has not yet been systematically resolved.

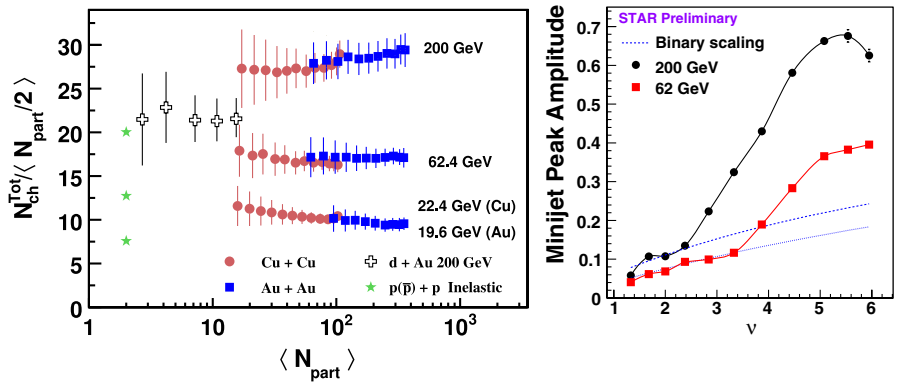

FIG. 5 (color online). Left panel: PHOBOS data [28] on an integrated number of charged particles, scaled by $N_{\mathrm{part}}/2$, in p + p, d + Au, Cu + Cu, and Au + Au collisions as a function of centrality. The uncertainty of N_{part} has been included in the error bars. Right panel: The height of the ridge as a function of the number of mean binary collisions per nucleon. The data are from the STAR Collaboration [30,32] at the two collision energies shown in the figure.

trapped surfaces at different impact parameters and collision energy. We observe a critical impact parameter within the range of energy we explored. The phenomenon is analogous to the critical behavior found in flat space [18–20], the difference being that the critical trapped surface depends both on the collision energy and the nucleus size. We found that the dependence is approximately given by a power law. Furthermore, the shape of the critical trapped surface gets elongated in spherical coordinates as the collision energy grows. We also discussed in the preceding subsection that grazing heavy ion collisions also seem to suggest a rapid switch to another dynamics, without equilibration. The exact cause of this jump will be clarified in future studies.

We also studied wall-to-wall collision of shock waves as a simple version of the problem. The wall is sourced by a delta function at a certain initial scale z_0. We believe it is a more reasonable initial condition than those used by Grumiller and Romatschke [13], and it will be used in the future following their method to study the initial stage.

The applicability and limitation of this approach are discussed. We claim it is more realistic to adopt a partonic picture in the initial stage and only switch to an effective gravity treatment at some time *after* collision, when the coupling becomes strong enough. However, we argue that the observed critical phenomenon is still relevant for heavy ion collisions, where there also seems to be a rapid change of the collision regime as a function of the impact parameter.

Finally, we would like to mention a very recent work by Alvarez-Gaume *et al.* [31], who discussed another extension of the problem. They considered central collision of shock waves sourced by certain nontrivial matter distribution in the transverse space. They, in particular, discussed the critical phenomenon occurring as the shock wave reaches some diluteness limit and the formation of the trapped surface is no longer possible. It would obviously be interesting to study how the two forms of critical phenomena are related.

ACKNOWLEDGMENTS

We thank Silviu Pufu, Kevin Dusling, and Stanislav Srednyak for valuable discussions. S. L. would like to thank Tom Kuo and Huan Dong for help with the integral equations. Our work was partially supported by the U.S. DOE Grant No. DE-FG02-88ER40388 and No. DE-FG03-97ER4014.

Note added.—Horatiu Nastase had informed us about his early work [33] in which he also addressed noncentral gravitational collisions; see also the summary in [34]. His estimate of the critical impact parameter $b_c(E) \sim E^{1/6}$ at large E is quite different from the power law obtained by us, perhaps because we are not working at asymptotically large E. After the first version of our work, another work by the Princeton group [35] was posted, in which they address the noncentral collision case we discussed above. Gubser *et al.* have provided a detailed comparison of our numerical results with their analytical formula, observing excellent agreement between the two calculations.

[1] E. V. Shuryak, Prog. Part. Nucl. Phys. **53**, 273 (2004).E. V. Shuryak and I. Zahed, Phys. Rev. C **70**, 021901 (2004).E. Shuryak and I. Zahed, Phys. Rev. D **69**, 046005 (2004).

[2] J. M. Maldacena, Adv. Theor. Math. Phys. **2**, 231 (1998); Int. J. Theor. Phys. **38**, 1113 (1999).

[3] E. Witten, Adv. Theor. Math. Phys. **2**, 253 (1998).

[4] S. S. Gubser, I. R. Klebanov, and A. A. Tseytlin, Nucl. Phys. **B534**, 202 (1998).

[5] G. Policastro, D. T. Son, and A. O. Starinets, Phys. Rev. Lett. **87**, 081601 (2001).

[6] J. Casalderrey-Solana and D. Teaney, Phys. Rev. D **74**, 085012 (2006).

[7] S.-J. Sin and I. Zahed, Phys. Lett. B **608**, 265 (2005); H. Liu, K. Rajagopal, and U. A. Wiedemann, arXiv:hep-ph/0605178; C. P. Herzog, A. Karch, P. Kovtun, C. Kozcaz, and L. G. Yaffe, arXiv:hep-th/0605158; S. S. Gubser and A. Buchel, arXiv:hep-th/0605178; arXiv:hep-th/0605182; S.-J. Sin and I. Zahed, arXiv:hep-ph/0606049.

[8] E. Shuryak, Prog. Part. Nucl. Phys. **62**, 48 (2009).

[9] E. Shuryak, S. J. Sin, and I. Zahed, J. Korean Phys. Soc. **50**, 384 (2007).

[10] R. A. Janik and R. Peschanski, Phys. Rev. D **73**, 045013 (2006).

[11] S. Nakamura and S. J. Sin, J. High Energy Phys. 09 (2006) 020; Phys. Lett. B **608**, 258 (2005).

[12] M. P. Heller, R. A. Janik, and R. Peschanski, Acta Phys. Pol. B **39**, 3183 (2008).

[13] D. Grumiller and P. Romatschke, J. High Energy Phys. 08 (2008) 027.

[14] J. L. Albacete, Y. V. Kovchegov, and A. Taliotis, J. High Energy Phys. 07 (2008) 100.

[15] S. Lin and E. Shuryak, Phys. Rev. D **78**, 125018 (2008).

[16] P. M. Chesler and L. G. Yaffe, arXiv:0812.2053 [Phys. Rev. Lett. (to be published)].

[17] S. S. Gubser, S. S. Pufu, and A. Yarom, Phys. Rev. D **78**, 066014 (2008).

[18] D. M. Eardley and S. B. Giddings, Phys. Rev. D **66**, 044011 (2002).

[19] H. Yoshino and Y. Nambu, Phys. Rev. D **67**, 024009 (2003).

[20] E. Kohlprath and G. Veneziano, J. High Energy Phys. 06 (2002) 057.

[21] S. W. Hawking and R. Penrose, Proc. R. Soc. A **314**, 529 (1970).

[22] D. E. Berenstein, R. Corrado, W. Fischler, and J. M. Maldacena, Phys. Rev. D **59**, 105023 (1999).

[23] U. H. Danielsson, E. Keski-Vakkuri, and M. Kruczenski, J. High Energy Phys. 01 (1999) 002.

[24] J. Polchinski and M. J. Strassler, Phys. Rev. Lett. **88**, 031601 (2002).

[25] U. Gursoy and E. Kiritsis, J. High Energy Phys. 02 (2008) 032.

[26] U. Gursoy, E. Kiritsis, and F. Nitti, J. High Energy Phys. 02 (2008) 019.

[27] E. Shuryak, arXiv:0711.0004.

[28] G. I. Veres *et al.* (PHOBOS Collaboration), arXiv: 0806.2803.

[29] E. V. Shuryak, Phys. Rev. C **76**, 047901 (2007).

[30] A. Dumitru, F. Gelis, L. McLerran, and R. Venugopalan, Nucl. Phys. **A810**, 91 (2008).

[31] L. Alvarez-Gaume, C. Gomez, A. S. Vera, A. Tavanfar, and M. A. Vazquez-Mozo, J. High Energy Phys. 02 (2009) 009.

[32] M. Daugherity (STAR Collaboration), J. Phys. G **35**, 104090 (2008).

[33] K. Kang and H. Nastase, Phys. Rev. D **72**, 106003 (2005).

[34] H. Nastase, Prog. Theor. Phys. Suppl. **174**, 274 (2008).

[35] S. S. Gubser, S. S. Pufu, and A. Yarom, arXiv:0902.4062.